

# A Folic Acid-Modified Polymeric Nanoliposome for Tumor-Targeted Drug Delivery

Farzaneh Sadrykia<sup>1</sup> , Peyman Najafi Moghadam<sup>1</sup> , Hamed Hamishehkar<sup>2,3</sup> 

<sup>1</sup>Department of Organic Chemistry, Faculty of Chemistry, Urmia University, Urmia, 57153-165, Iran

<sup>2</sup>Drug Applied Research Center, Tabriz University of Medical Sciences, Tabriz, Iran

<sup>3</sup>New Material and Green Chemistry Research Center, Khazar University, 41 Mehseti Street, Baku, AZ1096, Azerbaijan

## ARTICLE INFO

### Article History:

**Received:** July 2, 2025

**Revised:** September 8, 2025

**Accepted:** September 30, 2025

**ePublished:** April 30, 2026

### Keywords:

Doxorubicin, Folic acid,  
Polymeric nanoliposome,  
Targeted drug delivery

## Abstract

**Background:** Nowadays, scientists are trying to design a developed carrier for delivering drugs specifically to cancerous cells. This study aimed to design the poly (acrylamide-maleic anhydride)/(FA & TPGS) coated nanoliposome (P(AAm-MA)/(FA & TPGS) NL) as an FA-modified targeted drug delivery system.

**Methods:** The P(AAm-MA)/(FA & TPGS) copolymer was synthesized via free radical polymerization of AAm and MA, followed by chemical grafting of FA-NH<sub>2</sub> and TPGS-SS-NH<sub>2</sub>. Also, the nanoliposome (NL) was prepared by the thin lipid film hydration method and the Doxorubicin (DOX) was encapsulated into the core of nanoliposome during lipid bilayer formation. After that, the copolymer was used to coat the NL in order to prepare P(AAm-MA)/(FA & TPGS) NL. The cytotoxicity of DOX-loaded P(AAm-MA)/(FA & TPGS) NL, pure DOX and blank P(AAm-MA)/(FA & TPGS) NL against MCF-7 were measured by MTT assay. The intracellular uptake of free DOX and DOX-loaded P(AAm-MA)/(FA & TPGS) NL against MCF-7 was studied using a fluorescence microscope.

**Results:** The P(AAm-MA)/(FA & TPGS) copolymer was initially investigated by FT-IR, then the TEM analysis of P(AAm-MA)/(FA & TPGS) NL was performed, and showed that the copolymer formed a thin layer around liposomal vesicles. Also, the TEM and DLS results confirmed the preparation of P(AAm-MA)/(FA & TPGS) NL with less than 100 nm diameter. The zeta potential results confirmed the coating of NL with copolymer by electrostatic interactions. The DOX-loaded P(AAm-MA)/(FA & TPGS) NL exhibited enhanced cellular uptake through FA-mediated endocytosis. The efficiency of DOX-loaded P(AAm-MA)/(FA & TPGS) NL against MCF-7 was verified by MTT, and exhibited higher cytotoxicity of the DOX-loaded P(AAm-MA)/(FA & TPGS) NL compared to pure DOX.

**Conclusion:** Overall, the P(AAm-MA)/(FA & TPGS) NL controlled MCF-7 cells' growth because of its enhanced cellular uptake via FA-mediated endocytosis. Thus, the prepared nanoliposome carrier can be a suitable choice for inhibiting the growth of cancer cells.

## Introduction

Cancer is a disease caused by the uncontrolled growth of cells in the body. Chemotherapy is one of the common methods of cancer treatment. The use of common chemotherapy agents is associated with serious problems such as drug resistance and non-specificity of medications. In new cancer treatment methods, the side effects of antitumor drugs have been reduced by delivering the drug specifically to tumor cells.<sup>1</sup>

Drug carrier molecules are designed to deliver drugs specifically to target sites. Site-specific drug delivery is an interesting alternative to chemotherapy. Smart nanocarriers can respond to various stimuli such as pH, temperature, light, magnetic field, ultrasound, enzymes, oxidation, etc. Stimuli-responsive nanocarriers release their drug at the specific location depending on their smartness. Thermo-responsive polymers are a class of

smart materials that change their properties, such as solubility or composition, in response to temperature. These materials have attracted attention from the scientific community due to their potential applications in drug delivery devices and pharmaceuticals.<sup>2</sup> Ligand targeted nanocarriers use the ligand-receptor technique in order to locate the target sites such as cancer cells. Cancer cells and normal cells differ in their cell surface receptors. Cancer cells show the overexpression of folic acid (FA) receptors on their surface. So, the drug-loaded nanocarriers are modified with FA targeting ligands. These ligands can identify their matching target that is overexpressed on the surface of the cancer cell. Also, some other ligands such as peptides and antibodies can be used for this purpose. Ligand-targeted liposomes are suitable drug carriers made of phospholipid bilayers surrounding an aqueous core.<sup>3-13</sup> The nanotechnology based drug carriers have

\*Corresponding Author: Peyman Najafi Moghadam, Emails: [p\\_najafi27@yahoo.com](mailto:p_najafi27@yahoo.com); [p.najafi@urmia.ac.ir](mailto:p.najafi@urmia.ac.ir)

© 2026 The Author(s). This is an open access article and applies the Creative Commons Attribution Non-Commercial License (<http://creativecommons.org/licenses/by-nc/4.0/>). Non-commercial uses of the work are permitted, provided the original work is properly cited.

developed drug treatment by increasing the duration of drug retention in the bloodstream and reducing its side effects via maintaining effective drug concentration in the body.<sup>14,15</sup> Metal nanoparticles, such as silver (Ag), copper (Cu), and gold (Au), possess distinctive characteristics that make them valuable in cancer treatment. These nanoparticles are used as drug carriers. They also actively participate in therapeutic processes such as inducing apoptosis, which is crucial for the eradication of tumor cells.<sup>16</sup> In recent years, various drug nanocarriers have developed for targeted delivery of drugs to the tumor environment. Alireza Motavalizadehkakhky et al. used lipid-based FA conjugated and chitosan modified structures as a promising nanocarrier for drug delivery to cancer cells.<sup>17</sup> There have been many reports on the use of polymers in tissue engineering and drug delivery systems.<sup>18,19</sup> For example, in a research project, iron oxide ( $\text{Fe}_3\text{O}_4$ ) nanoparticles coated with a hyperbranched polyglycerol polymer and FA successfully used as targeted anticancer drug delivery system.<sup>20</sup> In addition to being used as carriers in drug delivery systems, polymer-coated nanoparticles are also used for magnetic resonance and fluorescence imaging. As an example, nanoparticles based on manganese ferrites coated with nitrogen-doped carbon dots, are used for dual-mode magnetic resonance and fluorescence imaging of cancerous tumors *in vivo*.<sup>21</sup>

Polymeric nanocarriers are known to deliver drugs specifically to cancer cells due to their ability to be modified by targeting agents.<sup>22</sup> Water-soluble monomers like maleic anhydride and acrylamide derivatives are used as suitable options for preparing polymeric carriers. Zakir M.O. Rzaev et al. prepared poly (N-isopropyl acrylamide-co-maleic anhydride) based copolymer with potential biomedical applications.<sup>23</sup> The D- $\alpha$ -tocopheryl polyethylene glycol 1000 succinate (TPGS) is a water-soluble and safe form of vitamin E. The TPGS as a polyethylene glycol (PEG)-based polymer molecule is known to overcome drug resistance with inhibition of the P-glycoprotein efflux pump, which is responsible for removing foreign agents out of tumor cells. The inhibition of P-glycoprotein efflux pump elevates the drug intracellular accumulation, and leads to increased therapeutic effects of the drug.<sup>24-26</sup> Si-Shen Feng et al. synthesized TPGS-doxorubicin (DOX)-FA conjugate carrier for targeted chemotherapy using the FA moiety in order to reduce the drug side effects.<sup>24</sup>

The liposomal nanocarriers are one of the attractive systems for targeted drug delivery due to their phospholipid bilayers surrounding an aqueous core. So, they are suitable molecules for encapsulating and delivering both hydrophilic and hydrophobic drugs to specific target site with reduced side effects.<sup>3,27</sup> Therefore, designing nanoliposomes combined with novel FA-containing polymers as tumor-targeted drug delivery systems could be an attractive approach. In this method, the FA targeting agent is used to overcome the non-specific delivery of drugs to tumor cells.

So far, researchers have conducted studies on designing targeted liposomal nanocarriers to deliver the hydrophilic anticancer DOX drug specifically to tumor cells.<sup>28</sup> Also, Yihui Deng et al. synthesized a sialic acid-cholesterol conjugate modified liposome with improved antitumor activity for targeted delivery of epirubicin to tumor-associated macrophages.<sup>29</sup> Furthermore, Jong-II Park et al. prepared a liposomal carrier containing cholesterol and mitochondria-penetrating peptide for targeted delivery of antimycin A to A549 cancer cells.<sup>30</sup> Saman Ahmad Nasrollahi et al. designed a nano liposomal topical emulgel formulation for the delivery of ruxolitinib in autoimmune skin disorders.<sup>31</sup>

The utility of nanoliposomes to deliver anticancer drugs to tumor cells may be limited by the body's immune system. So they need to be modified or functionalized to make them avoid the cleansing process of the body's immune system and achieve the developed targeted drug delivery systems.<sup>3</sup> Therefore, in this research work, we attempted to prepare a novel FA-functionalized nano liposomal carrier in order to overcome the non-specific drug delivery to tumor cells. Hence, this study aimed to design an FA-modified targeted drug delivery system that utilizes the ligand-receptor technique to locate the cancer cell and thus overcome the immune system.

In this research work, we design the synthetic procedure for the preparation of the poly (acrylamide-maleic anhydride-)/(FA & TPGS) coated nanoliposome (P(AAm-MA)/(FA & TPGS) NL) as an FA-modified targeted drug delivery system. For this purpose, the P(AAm-MA)/(FA & TPGS) copolymer was synthesized via free radical polymerization of AAm and MA, followed by chemical grafting of amine-functionalized FA-NH<sub>2</sub> and TPGS-SS-NH<sub>2</sub>. Also, the lecithin-based nanoliposome (NL) was prepared by the thin lipid film hydration method, and the hydrophilic DOX drug was encapsulated into the aqueous core of the nanoliposome during lipid bilayer formation. After that, the positively charged P(AAm-MA)/(FA & TPGS) copolymer was used to coat the negative surface of the lecithin-based NL in order to prepare the developed P(AAm-MA)/(FA & TPGS) NL. Finally, the efficiency of prepared DOX-loaded P(AAm-MA)/(FA & TPGS) NL against MCF-7 cancer cells was verified by MTT assay and cellular uptake experiment.

## Methods

### Materials

Acrylamide (AAm) and maleic anhydride (MA) monomers, FA, ethylene diamine, azobisisobutyronitrile (AIBN), 1,1'-carbonyldiimidazole (CDI), cystaminium dihydrochloride, triethylamine, N, N'-dicyclohexylcarbodiimide (DCC), tween 80, N-hydroxysuccinimide (NHS), tetrahydrofuran (THF), acetonitrile, Dimethyl sulfoxide (DMSO), methanol, dioxane, n-hexane, dimethylformamide (DMF), ethanol, diethyl ether, and pyridine were obtained from Merck. The DOX drug was purchased from Actoverco Pharmaceutical

Company. The Lecithin was purchased from Maharashtra, India. The TPGS and 3-(4, 5-dimethylthiazol-2-yl)-2, 5-diphenyltetrazolium bromide (MTT) were purchased from Sigma-Aldrich, and the MCF-7 was purchased from the cell bank of Pasteur Institute (Tehran, Iran). Fetal bovine serum (FBS), penicillin/streptomycin, and RPMI-1640 were purchased from Gibco (Carlsbad, USA).

### Synthesis of P(AAm-MA)

The P(AAm-MA) copolymer was synthesized via free radical polymerization, similar to the published method,<sup>32</sup> with minimal modification (Figure 1c). A mixture of AAm (2 g, 28.1 mmol), MA (2.753 g, 28.1 mmol), and dried THF (50 mL) was poured into a 100 mL two-necked flask with a nitrogen inlet and outlet. The solution was bubbled with inert gas for 18 min. Then, AIBN (0.138 g, 0.843 mmol) was added under an inert gas atmosphere to the solution. The mixture was stirred under reflux conditions for about 23 h and then cooled down to room temperature. Afterward, the product was added dropwise to excess cold n-hexane to form a precipitate. The white

precipitate was separated via centrifugation, washed two times with methanol, and dried at 60°C overnight to get P(AAm-MA) copolymer.

### Synthesis of FA-NH<sub>2</sub> and TPGS-SS-NH<sub>2</sub> Grafts

#### Synthesis of TPGS-SS-NH<sub>2</sub>

The amine-terminated TPGS (TPGS-SS-NH<sub>2</sub>) was synthesized from the TPGS in two steps using a published procedure with slight modification (Figure 1a).<sup>33</sup> In the first step, TPGS was activated by the CDI activating agent. The carbonyl group of CDI reacts with the hydroxyl group of TPGS, forming an imidazole carbamate intermediate (TPGS-CDI). This activated intermediate can then be used in further reactions, such as conjugation with other molecules like amines. Briefly, CDI (2.13 g, 13.13 mmol) and TPGS (4 g, 2.64 mmol) were dissolved in dioxane separately. Then, TPGS solution was added dropwise to CDI solution, and stirred for 20h at 37 °C. Afterward, CDI-activated TPGS (TPGS-CDI) was precipitated in excess cold n-hexane and washed with the same solvent. The resultant precipitate remained overnight at room

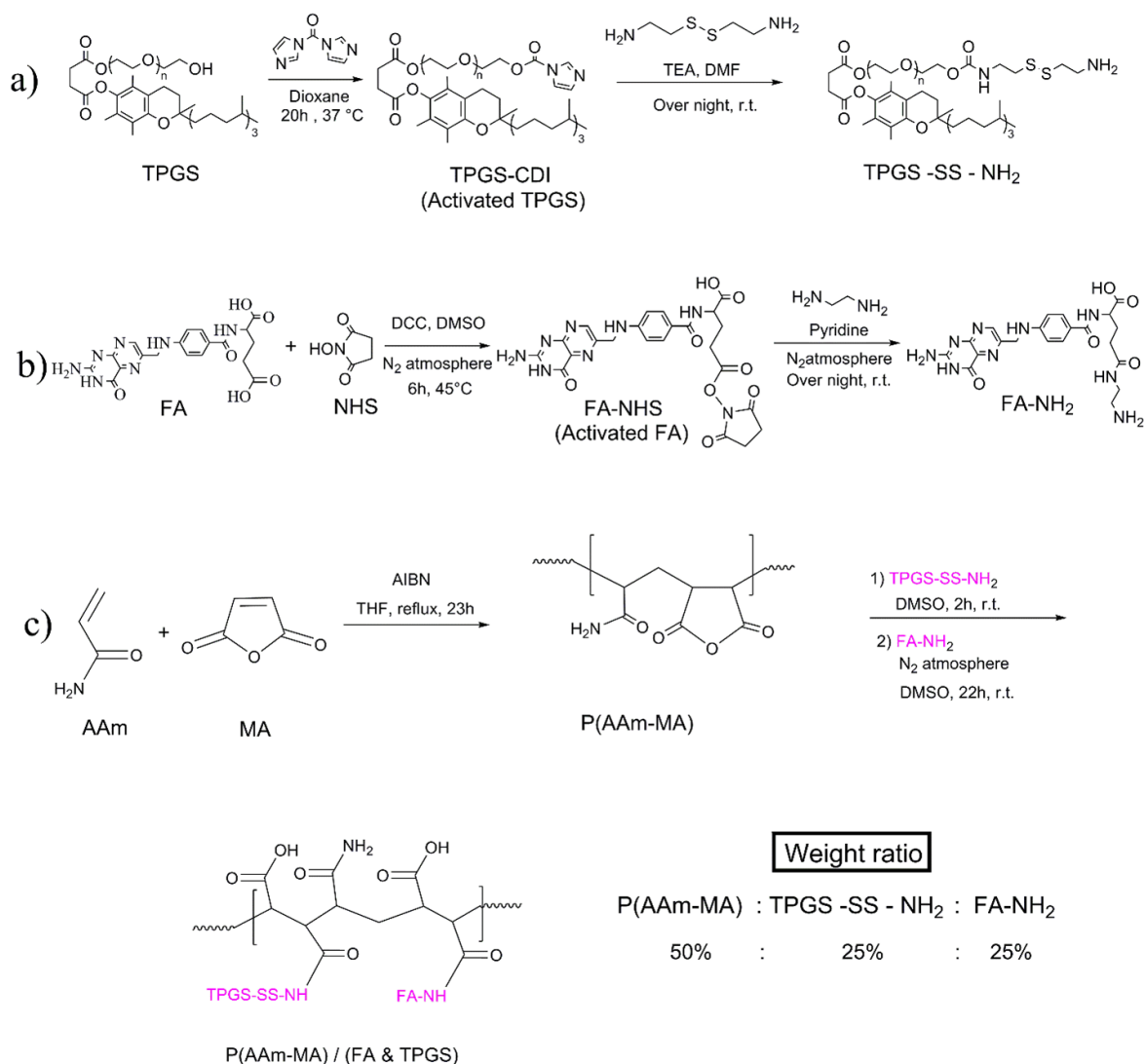


**Figure 1.** Synthesis of a) the amine-terminated TPGS (TPGS-SS-NH<sub>2</sub>), b) the amine-functionalized FA (FA-NH<sub>2</sub>), c) the P(AAm-MA) and P(AAm-MA)/(FA & TPGS) copolymers

temperature to dry completely.

In the second step, TPGS-CDI was converted to TPGS-SS-NH<sub>2</sub>. Briefly, cystaminium dihydrochloride (1.9 g, 12.5 mmol), DMF (20 ml), and triethylamine (4.3 ml, 30.9 mmol) were added to a flask. Afterward, the TPGS-CDI (4 g, 2.5 mmol) was dissolved in DMF separately and added dropwise to the cystaminium dihydrochloride solution. The resultant was kept under stirring at room temperature overnight. Then, the reaction mixture was dialyzed (MWCO of dialysis bag is 1000Da) against distilled water: ethanol (1:1, v/v) for 24h and then distilled water for another 24h. Afterward, the content of the dialysis tube was freeze-dried to obtain TPGS-SS-NH<sub>2</sub>.

#### Synthesis of FA-NH<sub>2</sub>

The amine-functionalized FA (FA-NH<sub>2</sub>) was synthesized using a published procedure,<sup>12</sup> with minimal modification (Figure 1b). At first, the carboxylic acid group of FA was activated by NHS and DCC, making it reactive towards the amine group of ethylene diamine. DCC reacts with the carboxylic acid group of FA, forming an unstable O-acylisourea intermediate. Then, the NHS reacts with the O-acylisourea, forming a more stable NHS ester (FA-NHS). The reaction also produces 1, 3-dicyclohexylurea as a by-product, which can be removed by filtration. The activated ester (FA-NHS) is more susceptible to nucleophilic attack by the amine group of ethylene diamine, leading to the formation of the desired amide bond and the synthesis of FA-NH<sub>2</sub>. Briefly, FA (4 g, 9.1 mmol), NHS (2.1 g, 18.2 mmol), and DCC (2.2 g, 10.7 mmol) were dissolved in DMSO (50ml) and stirred under inert gas (N<sub>2</sub>) in the dark at 45 °C for six hours. The obtained mixture was filtered to remove 1, 3-dicyclohexylurea by-product. The resultant solution was reacted with ethylene diamine (7.1 g, 118.1 mmol) in the presence of pyridine (4.5 g, 57 mmol) under inert gas in dark at room temperature overnight. The product was dropped into excess acetonitrile; the precipitate was collected and washed three times with diethyl ether. Then, the precipitate was dried at 35 °C in the oven to get yellow FA-NH<sub>2</sub> powder.

#### Synthesis of P(AAm-MA)/(FA & TPGS)

The P(AAm-MA)/(FA & TPGS) copolymer was synthesized by the chemical graft reaction of FA-NH<sub>2</sub> and TPGS-SS-NH<sub>2</sub> molecules on P(AAm-MA) (Figure 1c). In this modification reaction, the P(AAm-MA), TPGS-SS-NH<sub>2</sub>, and FA-NH<sub>2</sub> were used at weight ratios of 50%, 25%, and 25%, respectively. Briefly, at first, P(AAm-MA) (2 g) and TPGS-SS-NH<sub>2</sub> (0.5 g) were dissolved in DMSO separately. Then, the TPGS-SS-NH<sub>2</sub> and P(AAm-MA) solutions were mixed and stirred for two hours at 25°C. The resultant was mixed with the solution of FA-NH<sub>2</sub> (0.5 g) in DMSO and stirred under inert gas (N<sub>2</sub>) in the dark at room temperature for 22h. The product was freeze-dried and then washed with n-hexane. Finally, the obtained P(AAm-MA)/(FA & TPGS) product was dried at 35 °C for 12h.

#### Preparation of Nanoliposome (NL)

The NL was prepared by the thin lipid film hydration method as described by Hadi Almasi et al.<sup>34</sup> with minimal modification. Briefly, lecithin phospholipid (90 mg) and a drop of Tween 80 were added to 96% ethanol solvent (10 ml) and stirred to dissolve completely. Then, the resulting solution was transferred to a round-bottom flask and rotated on a rotary evaporator at about 55 °C for 20 min in order to form a thin layer at the bottom of the flask. Afterwards, the resulting lipid film was hydrated with distilled water (10 ml) on the rotary evaporator at about 60 °C for 10 min. Then, the obtained solution was homogenized at 20000 rpm in 60°C for 20 min in order to prepare NL suspension.

#### Preparation of P(AAm-MA)/(FA & TPGS) Coated Nanoliposome: P(AAm-MA)/(FA & TPGS) NL

The P(AAm-MA)/(FA & TPGS) NL was prepared by surface modification of NL (Figure 2). For this purpose, at first, bare NL was prepared by the thin lipid film hydration method mentioned above. Then, the P(AAm-MA)/(FA & TPGS) polymer (75 mg) was dissolved in distilled water (1 ml). Afterwards, this polymer solution was added dropwise to the prepared NL suspension, using a 1 ml syringe, and stirred for two h. The targeted P(AAm-MA)/(FA & TPGS) NL is achieved through the electrostatic interaction of the oppositely charged P(AAm-MA)/(FA & TPGS) polymer around the NL surface.

#### Characterization

Fourier transform infrared (FT-IR) spectra of the samples were obtained with an FT-IR spectrometer (Tensor 27, Bruker, Germany) using KBr powder. The proton nuclear magnetic resonance (<sup>1</sup>H-NMR) spectra of the samples were recorded on a Varian NMR spectrometer (Varian Inova 500 MHz, CA). The thermo gravimetric analysis (TGA) was carried out (STAPT1000, Linseis, Germany) with a 10°C/min heating rate (from 25 to 700 °C) under a nitrogen atmosphere. The sample morphology was detected using a field emission scanning electron microscope (FE-SEM) instrument (Hitachi S4160, Japan) at a voltage of 20 kV. Moreover, the morphology of the samples was studied by transmission electron microscopy (TEM). To prepare the sample for TEM, a drop of the diluted sample was placed on a carbon-coated copper grid. After removing the excess solution, the sample was stained with uranyl acetate and photographed (Zeiss-Leo 906, Germany) at an accelerating voltage of 120 kV. The zeta and particle sizes of samples were determined using dynamic light scattering (DLS, Nano ZS, ZEN 3600, Malvern).

#### Drug Loading and Encapsulation Efficiency

Loading of the hydrophilic anticancer DOX drug into P(AAm-MA)/(FA & TPGS) NL was performed during its preparation. So, the preparation steps of DOX-loaded P(AAm-MA)/(FA & TPGS) NL were similar to that

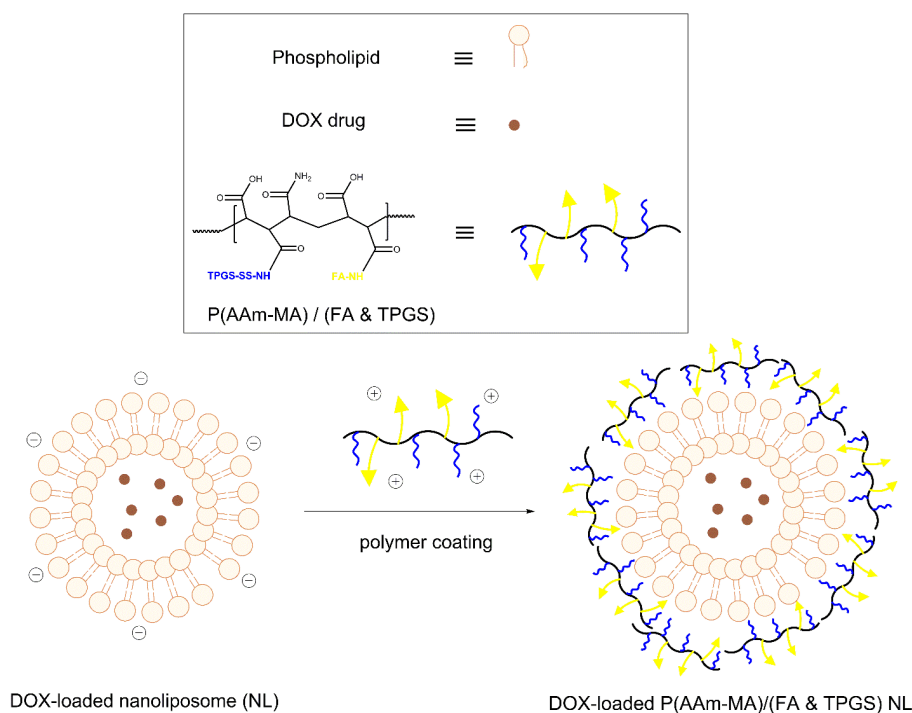


**Figure 2.** Synthesis of P(AAm-MA)/(FA & TPGS) coated nanoliposome (NL) as targeted drug delivery system

of P(AAm-MA)/(FA & TPGS) NL, except that, in the hydration step, instead of adding 10 ml distilled water, the following procedure was performed: The DOX drug (1mg) was dissolved in 1ml of distilled water and added to the lipid film of flask on a rotary evaporator at 60 °C. After 1 min, an additional distilled water (9 ml) was added and allowed to rotate for 9 min.

Furthermore, before the aforementioned P(AAm-MA)/(FA & TPGS) polymer addition step, the resultant product was dialyzed (MWCO of dialysis bag is 1000Da) against distilled water for one h to remove the unloaded DOX drug.

The incorporated amount of DOX in P(AAm-MA)/(FA & TPGS) NL was determined using a UV-Vis spectrophotometer (Ultrospec 2000, Pharmacia Biotech, UK) at 480 nm. The encapsulation efficiency (EE%) and the loading capacity (LC%) were calculated as following equations (1) and (2).

$$EE\% = [\text{weight of DOX in NL}] / [\text{weight of DOX fed}] \times 100 \quad (1)$$

$$LC\% = [\text{weight of DOX in NL}] / [\text{weight of DOX-loaded NL}] \times 100 \quad (2)$$

#### **In Vitro Drug Release Study**

The *in vitro* drug release from DOX-loaded P(AAm-MA)/(FA & TPGS) NL with a 98.8 µg/ml DOX concentration was studied in pH=5.3 phosphate buffer solution (PBS) at 40 °C as the release medium, in order to simulate the tumor cell environment. Briefly, the prepared DOX-loaded P(AAm-MA)/(FA & TPGS) NL was transferred to the dialysis bag (MWCO=1000 Da). Then, the bag

was immersed in 10 mL of release medium and kept in a shaker-incubator (Unimax1010 Heidolph, Germany) at 40°C and 140 rpm. The sampling was done by withdrawing the 1 mL release medium at predetermined time intervals and replacing it with the same volume of fresh medium. The released DOX content was quantified using a UV-Vis spectrophotometer at 270 nm, and the results of the release percentage were obtained according to equation (3) in terms of cumulative release as a function of time:

$$\text{Cumulative DOX release\%} = [\text{cumulative amount of released DOX from the NL at time } t] / [\text{the initial amount of DOX in the NL}] \times 100 \quad (3)$$

#### **Cell Culture**

The human breast cancer MCF-7 cells were cultured in RPMI-1640 containing 100 mg/mL streptomycin, 100 units/mL penicillin, and 10% FBS at a 37°C incubator with 5% CO<sub>2</sub> and 97% humidity.

#### **In Vitro Cytotoxicity Assay**

The cytotoxicity of DOX-loaded P(AAm-MA)/(FA & TPGS) NL, pure DOX and blank P(AAm-MA)/(FA & TPGS) NL against MCF-7 cells were measured by MTT assay. The cells were seeded in 96-well plates at a density of 10<sup>4</sup> cells per well. After incubation for 48 h, the cells were treated with different concentrations of the formulations mentioned above. Each experiment was carried out in triplicate. Then, the treated cells and untreated cells (negative control) were incubated for 48 h. After that, the medium was removed, and then 200µl fresh medium containing MTT powder (5 mg/ml) was added to each well and incubated for four hours. Afterward, the

medium was removed and replaced with DMSO (200 $\mu$ l) to dissolve formazan crystals, and the absorbance of formazan solution was measured by a microplate reader (BioTek, ELx808, USA) at 570 nm.

### Cellular Uptake Study

The intracellular uptake of DOX-loaded P(AAm-MA)/(FA & TPGS) NL and free DOX against MCF-7 cells was tracked by a fluorescence microscope (BX50, Olympus, Japan) due to the auto-fluorescent property of DOX drug. The MCF-7 cells were seeded on coverslips in a 6-well plate at a density of  $10^4$  cells per well and incubated for 48 h. Afterward, the cells were treated with DOX-containing samples (DOX-loaded P(AAm-MA)/(FA & TPGS) NL and free DOX) at the  $IC_{50}$  concentration. After incubation for three h, the medium was removed, the cells were washed twice with PBS (pH=7.4), and then, the coverslips were fixed onto the glass slides. Then, the uptake of targeted DOX-loaded P(AAm-MA)/(FA & TPGS) NL and free DOX by MCF-7 cells was observed using fluorescence microscopy.

## Results and Discussion

### Preparation of Targeted P(AAm-MA)/(FA & TPGS) Coated Nanoliposome: P(AAm-MA)/(FA & TPGS) NL

The FA-modified nano liposomal carriers are a suitable choice for targeted drug delivery. So, in this study, the FA-containing P(AAm-MA)/(FA & TPGS) copolymer is used to coat a lecithin-based nano liposomal carrier. In this work, in order to prepare the developed targeted P(AAm-MA)/(FA & TPGS) NL, at first, the P(AAm-MA)/(FA & TPGS) copolymer was synthesized via typical free radical polymerization of AAm and MA, followed by chemical grafting of FA-NH<sub>2</sub> and TPGS-SS-NH<sub>2</sub> (Figure 1c). Also, the lecithin-based NL was prepared by the thin lipid film hydration method, and the hydrophilic DOX drug was

encapsulated into the aqueous core of the NL during lipid bilayer formation. After that, the resultant FA-containing P(AAm-MA)/(FA & TPGS) copolymer was used for the surface coating of the prepared NL carrier (Figure 2). So, the obtained P(AAm-MA)/(FA & TPGS) NL is designed for use in the targeted delivery of antitumor DOX drug because of its enhanced cellular uptake via FA receptor-mediated endocytosis (Figure 3). In this method, the novel liposomal formulation combined with FA-containing polymer overcomes the non-specific drug delivery to tumor cells. The mechanism of cellular uptake for prepared nanoliposomes involves the binding of FA on the liposome surface to FA receptors overexpressed on tumor cell membranes. Then the nanoliposome is internalized via endocytosis, forming an endosome.<sup>35</sup>

### Structural Characterization

#### Fourier Transform Infrared Spectroscopy (FT-IR)

The FT-IR spectroscopy is an important method for determining chemical structure. So, FT-IR spectra of P(AAm-MA) and P(AAm-MA)/(FA & TPGS) are shown in Figure 4 to evaluate their chemical structure. In Figure 1a, which is related to the FT-IR of P(AAm-MA) copolymer, the peaks at 1652, 1715 and 1802  $cm^{-1}$  are related to repeated groups of MA. The AAm carbonyl peak appears at around 1652  $cm^{-1}$ , which overlaps with the MA peaks. Also, the peak at 3351 is related to NH<sub>2</sub> of amide in the P(AAm-MA) copolymer, which overlaps with the OH stretching vibration.

Figure 4b shows the FT-IR spectra of P(AAm-MA)/(FA & TPGS) copolymer. In Figure 4b, the peaks at 1673 and 1712  $cm^{-1}$ , which correspond to the carbonyl groups of amides and carboxylic acids, respectively, are stronger than in the P(AAm-MA) spectrum. These peaks are good evidence that FA-NH<sub>2</sub> and TPGS-SS-NH<sub>2</sub> have been successfully grafted to P(AAm-MA). Also, the broad band

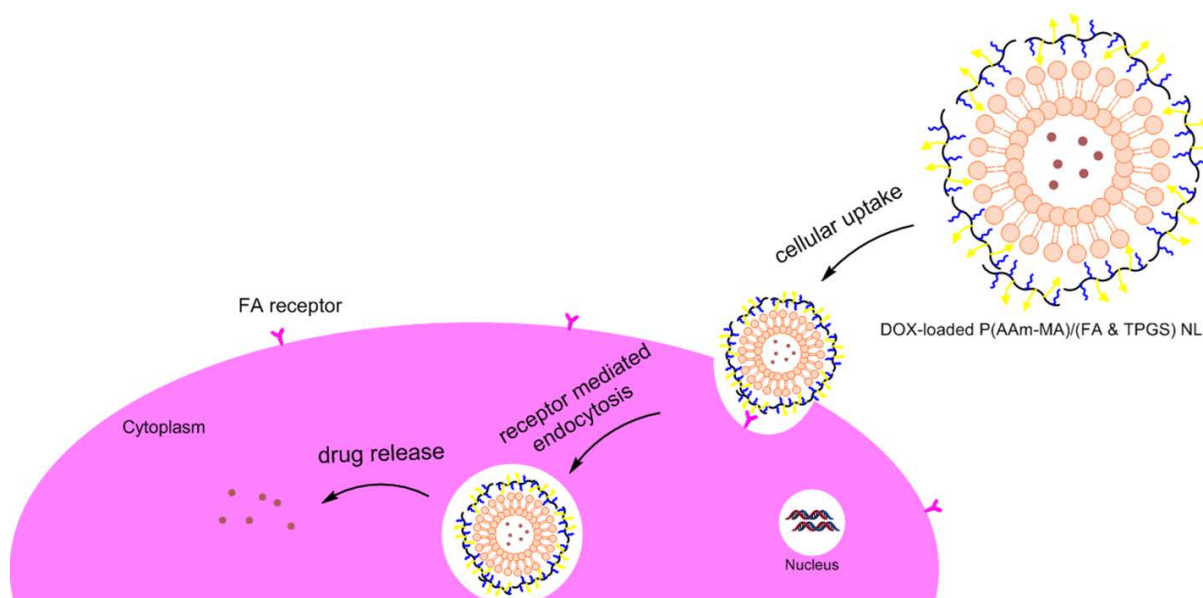


**Figure 3.** The intracellular uptake of the DOX-loaded P(AAm-MA)/(FA & TPGS) nanoliposome (NL) as targeted drug delivery system

at  $3363\text{ cm}^{-1}$  is related to the stretching vibration of OH, which overlaps with the  $\text{NH}_2$  peak of amide. It is clear that, the broad peak at  $3363\text{ cm}^{-1}$  compared to the P(AAm-MA) spectrum, is due to the increased hydrophilicity of the P(AAm-MA)/(FA & TPGS) after grafting of FA and TPGS on P(AAm-MA). The mentioned peaks in Figure 4b are good evidence of the successful grafting of FA-NH<sub>2</sub> and TPGS-SS-NH<sub>2</sub> to P(AAm-MA).

The amination of FA is characterized by FT-IR spectroscopy (Figure 5). The FA spectrum shows a C=O stretching vibration at  $1695.18\text{ cm}^{-1}$  and the characteristic

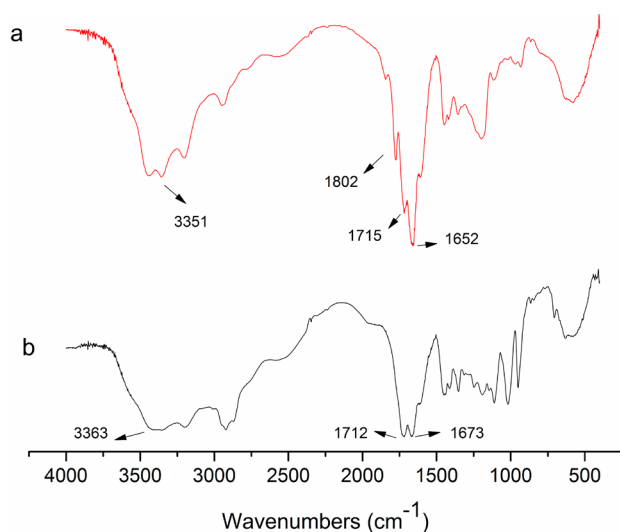


**Figure 4.** The FT-IR spectra of a) P(AAm-MA) and b) P(AAm-MA)/(FA & TPGS) copolymers

peak of the aromatic ring at  $1611\text{ cm}^{-1}$  (Figure 5a).

Figure 5b is related to the FT-IR spectrum of FA-NH<sub>2</sub>. The characteristic peak of the carboxyl group in Figure 5b, has become weaker and shifted to  $1681.54\text{ cm}^{-1}$  compared to the pure FA spectrum. This result indicates that the amination of FA has been done successfully.

#### Proton Nuclear Magnetic Resonance Spectroscopy (<sup>1</sup>H-NMR)

The <sup>1</sup>H-NMR spectroscopy was used to confirm the chemical structures of TPGS-SS-NH<sub>2</sub>. The <sup>1</sup>H-NMR spectra of TPGS and TPGS-SS-NH<sub>2</sub> are shown in Figure 6. As seen from the spectrum of TPGS, signals at 0.82 to 2.91 ppm correspond to various protons of the tocopheryl succinate unit in the TPGS. Also, the sharp signal at 3.52

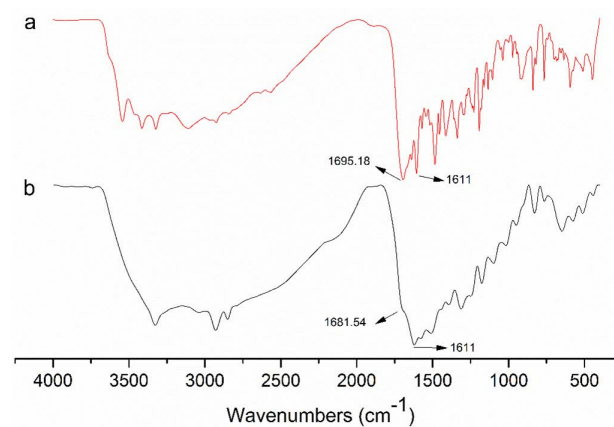


**Figure 5.** The FT-IR spectra of a) folic acid (FA) and b) aminated FA (FA-NH<sub>2</sub>)

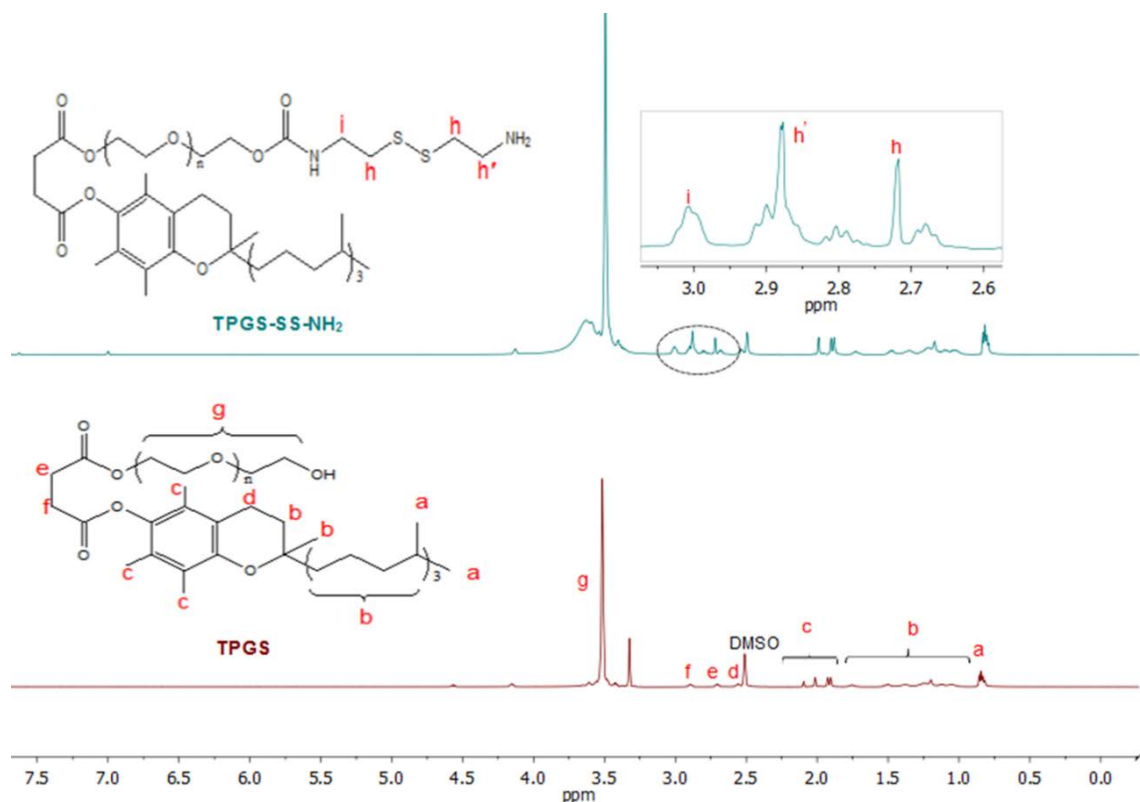


**Figure 6.** The <sup>1</sup>H-NMR spectra of TPGS and amine-terminated TPGS (TPGS-SS-NH<sub>2</sub>)

ppm corresponds to the methylene protons of the PEG moiety. At the spectrum of TPGS-SS-NH<sub>2</sub>, the new peaks at 2.72, 2.88, and 2.9 ppm emerge from -CH<sub>2</sub>- groups of the cystamide moiety. This result proves the successful synthesis of TPGS-SS-NH<sub>2</sub>.

#### Thermo Gravimetric Analysis (TGA)

The TGA was used to study the thermal properties of synthesized copolymers. The TGA thermograms of P(AAm-MA) and P(AAm-MA)/(FA & TPGS) copolymers are shown in Figure 7a and b, respectively. In the P(AAm-MA) thermogram curve, the first weight loss of about 3% up to 102 °C is related to the evaporation of adsorbed moisture. After that, the functional groups of the polymer degrade, followed by the degradation of the polymer backbone.

In the P(AAm-MA)/(FA & TPGS) thermogram, the first weight loss is attributed to moisture evaporation. Then, FA and TPGS grafts degrade, followed by the polymer backbone degradation process. The comparison of thermograms a and b in Figure 7 shows that the degradation process of P(AAm-MA)/(FA & TPGS) occurs at lower temperatures than that of P(AAm-MA); therefore, its thermal stability is lower than that of P(AAm-MA). Furthermore, the weight percentages of residue amounts (residue wt. %) at 700 °C for P(AAm-MA) and P(AAm-MA)/(FA & TPGS) are 27.3% and 10.6%, respectively. These findings show that grafting of TPGS and FA on P(AAm-MA) copolymer has been done successfully. It can also be seen in Figure 7 that the thermal stability of P(AAm-MA)/(FA & TPGS) is lower than that of P(AAm-

MA) at all temperatures, but the slopes of the P(AAm-MA) and P(AAm-MA)/(FA & TPGS) thermograms are almost similar at temperatures above 325 °C. This phenomenon indicates that in the P(AAm-MA)/(FA & TPGS) thermogram, the degradation of FA and TPGS grafts has occurred at temperatures below 325 °C, and the degradation of the polymer backbone - which has a similar slope in both P(AAm-MA) and P(AAm-MA)/(FA & TPGS) copolymers - has occurred at temperatures above 325 °C.

#### Field Emission Scanning Electron Microscopy (FE-SEM) Observations

The FE-SEM is an efficient method for assessing the morphology of materials. Figure 8(a and b) shows the FE-SEM images of P(AAm-MA) and P(AAm-MA)/(FA & TPGS) samples, respectively. As shown in Figure 8, the morphology of P(AAm-MA) has changed after being converted into P(AAm-MA)/(FA & TPGS) copolymer. Comparing images a and b in Figure 8 shows that the surface morphology of the P(AAm-MA) copolymer is smoother than that of P(AAm-MA)/(FA & TPGS), and in image b, pores with a size of about 200 nm are seen. In fact, after grafting of FA and TPGS on P(AAm-MA) in order to synthesize P(AAm-MA)/(FA & TPGS), the porosity increases, and a morphological change occurs.

Figure 9a and b show the FE-SEM and S-map of P(AAm-MA)/(FA & TPGS), respectively. The presence of S (shown by orange dots) in Figure 9b, can prove the grafting of TPGS-SS-NH<sub>2</sub> to the P(AAm-MA) copolymer.

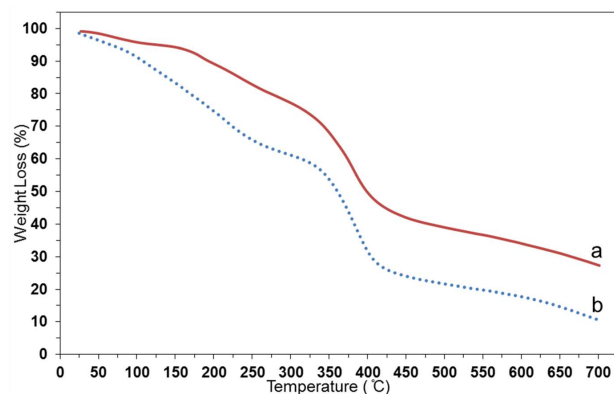


Figure 7. The TGA thermograms of a) P(AAm-MA) and b) P(AAm-MA)/(FA & TPGS) copolymers

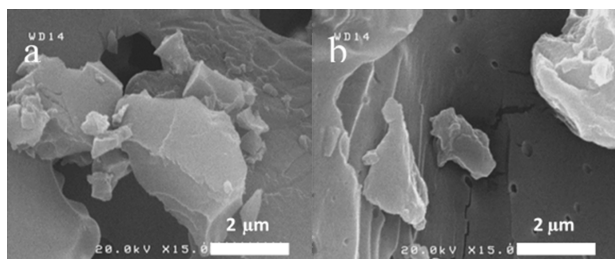


Figure 8. The FE-SEM images of a) P(AAm-MA) and b) P(AAm-MA)/(FA & TPGS) copolymers

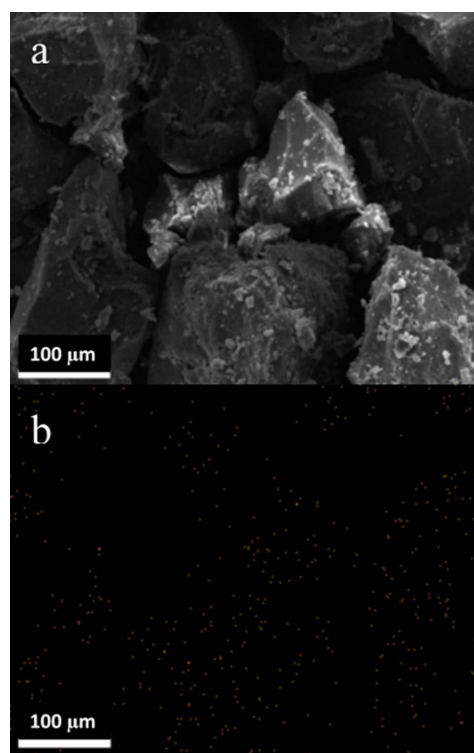


Figure 9. The a) FE-SEM and b) S-map of P(AAm-MA)/(FA & TPGS) copolymer

### Transmission Electron Microscopy (TEM)

Figure 10 shows the TEM image of the prepared P(AAm-MA)/(FA & TPGS) NL to study its structure. In Figure 10, a thin layer can be detected around some liposomal vesicles, indicating the successful surface coating of NL with the P(AAm-MA)/(FA & TPGS) copolymer. As indicated in Figure 10, the size of the prepared P(AAm-MA)/(FA & TPGS) NL is less than 100 nm.

### Dynamic Light Scattering (DLS)

The average particle size and zeta potential of the prepared NL and P(AAm-MA)/(FA & TPGS) NL were determined using DLS at 25 °C. As can be seen in Figure 11a and b, the average particle size of NL and P(AAm-MA)/(FA & TPGS)

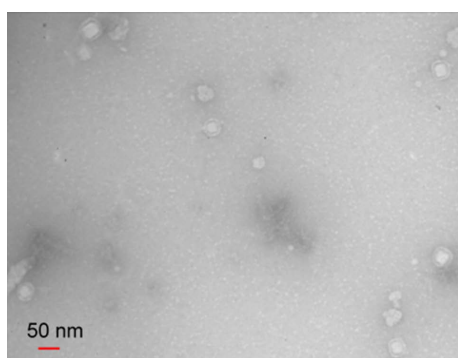


**Figure 10.** The TEM image of the P(AAm-MA)/(FA & TPGS) coated nanoliposome (NL)

NL is 50.21 and 85.42 nm, respectively. This finding proves the successful preparation of nano-sized liposomes. Also, according to Figure 11a and b, the successful coating of NL by the copolymer caused the size of P(AAm-MA)/(FA & TPGS) NL to be larger than that of bare NL.

Zeta potential is an essential factor that reveals the surface charge of nanoliposomes. As can be seen in Figure 11c and d, the zeta potential of NL and P(AAm-MA)/(FA & TPGS) NL is -26.0 and -14.8 mV, respectively. The outer negative heads of lecithin phospholipid bilayers are responsible for the negative charge of the prepared NL. According to Figure 11c and d, the negative charge of P(AAm-MA)/(FA & TPGS) NL decreases compared to bare NL. This phenomenon shows that the surface coating of NL with P(AAm-MA)/(FA & TPGS) copolymer is done by electrostatic interactions between the outer negative head of phospholipid bilayers and positively charged P(AAm-MA)/(FA & TPGS) coating.

### Drug Loading and In Vitro Release Study

In the liposome structure, the aqueous core is surrounded by a lipid bilayer, making it a good option for encapsulating and delivering both hydrophilic and hydrophobic drugs. Typically, hydrophilic drugs are loaded into the aqueous core of the liposome, while the hydrophobic drugs are loaded into the lipid bilayer.<sup>36</sup> So, in this study, the DOX, as an anticancer hydrophilic drug, was encapsulated into the aqueous core of the P(AAm-MA)/(FA & TPGS) NL

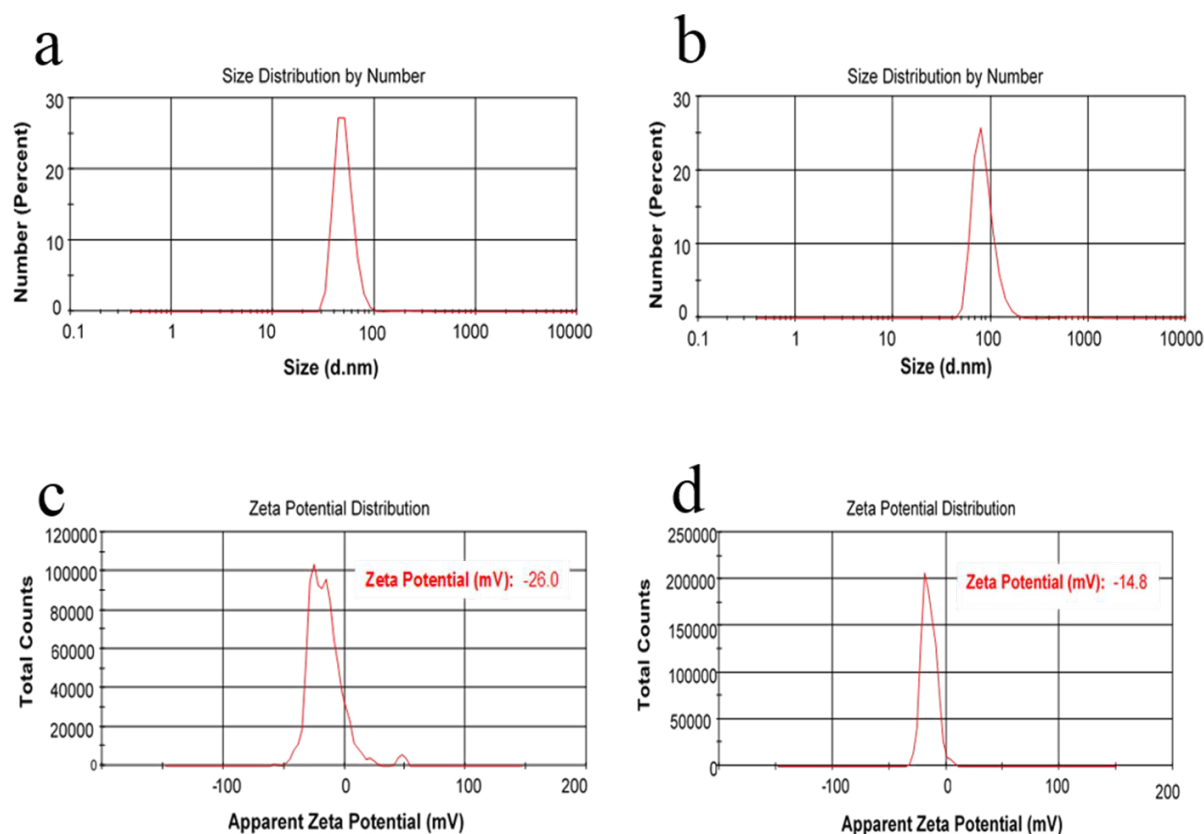


**Figure 11.** The a) average particle size of nanoliposome (NL), b) average particle size of P(AAm-MA)/(FA & TPGS) coated NL, c) zeta potential of NL and d) zeta potential of P(AAm-MA)/(FA & TPGS) coated NL by DLS

during lipid bilayer formation. The amounts of EE and LC for DOX-loaded P(AAm-MA)/(FA & TPGS) NL are 98.8% and 1.1% respectively.

The drug release from DOX-loaded P(AAm-MA)/(FA & TPGS) NL and free DOX under tumor-simulating conditions (pH=5.3 and 40 °C) is shown in Figure 12. According to Figure 12, in the tumor-simulated environment, free DOX has a rapid release, and 99.7% of the drug was released within a short time (12 h). In contrast, 66.5% of DOX drug encapsulated in the targeted NL was released within 48 h. So, comparing the release of free drug (free DOX) with encapsulated DOX in the NL indicates the controlled release capability of the prepared nanoliposomal system.

A pH-sensitive copolymer can be used to stimulate the breakdown of polymer-coated nanoliposomes in the pH of the tumor cell.<sup>37</sup> The drug release from DOX-loaded P(AAm-MA)/(FA & TPGS) NL under different pH conditions (pH=5.3 and pH=7.4) at 40 °C is shown in Figure 12. According to Figure 12, a faster release at pH=5.3 (tumor-simulated pH) compared to the slower release at pH=7.4 (physiological pH) confirms the pH-dependent performance of the system. Also, as seen in Figure 12, the cumulative amounts of drug released after 48 h for DOX-loaded P(AAm-MA)/(FA & TPGS) NL are 66.5% and 55.1% at pH=5.3 and 7.4 respectively. This finding further confirms the pH-dependent behavior of the prepared drug delivery system.

The P(AAm-MA)/(FA & TPGS) copolymer (as the pH-sensitive coating of P(AAm-MA)/(FA & TPGS) NL) becomes protonated after entering the cancer cell under the influence of its acidic environment. Then, P(AAm-MA)/(FA & TPGS) NL lyses by the influence of a strong positive charge, leading to rapid release of the drug into the cancer cell. This finding indicates that the targeted P(AAm-MA)/(FA & TPGS) NL, effectively releases the encapsulated drug under tumor-simulating conditions.

Therefore, the prepared targeted P(AAm-MA)/(FA & TPGS) NL is a suitable option for delivering the hydrophilic DOX drug into the cancer cell environment.

### In Vitro Cytotoxicity Assay

The cellular cytotoxicity of various formulations is

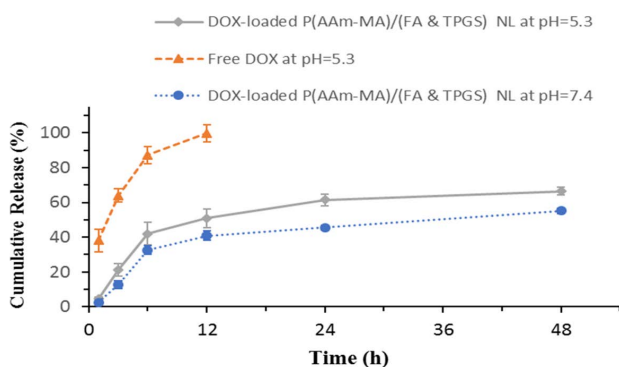


**Figure 12.** The cumulative drug release profile of free DOX at pH=5.3, DOX-loaded P(AAm-MA)/(FA & TPGS) nanoliposome (NL) at pH=5.3 and 7.4

measured by MTT assay (Figure 13). As shown in Figure 13, DOX-loaded P(AAm-MA)/(FA & TPGS) NL shows more toxicity to the MCF-7 cells than the pure DOX. Also, the IC<sub>50</sub> values of pure DOX and DOX-loaded P(AAm-MA)/(FA & TPGS) NL are 0.45 µg/ml and 0.19 µg/ml, respectively. This phenomenon confirms the higher cytotoxicity of the targeted drug-loaded P(AAm-MA)/(FA & TPGS) NL. According to the obtained results, the lower drug administration dose is used in DOX-loaded P(AAm-MA)/(FA & TPGS) NL compared to pure DOX for tumor growth control. The lower drug dose usage leads to a decrease in the side effects of drugs in high dosages.

The FA receptors are overexpressed in tumor cells.<sup>35</sup> The prepared FA-targeted nanoliposomes enhance drug delivery to cancer cells by exploiting the overexpression of FA receptors on cancer cell surfaces, leading to increased cellular uptake and cytotoxicity compared to free drug. The mechanism involves FA (as a targeting ligand on the nanoliposome surface) binding specifically to FA receptors on the cancer cell membrane, triggering endocytosis and internalization of the nanoliposome. Once inside the cell, the DOX drug is released, exerting its cytotoxic effect, while free drug uptake is less efficient and non-targeted. So, free DOX drug has less cellular accumulation. By selectively targeting MCF-7 cancer cells, FA-targeted nanoliposomes can potentially reduce the side effects associated with free DOX drug administration.

In this study, our team focused on targeting receptors of tumor cells by FA conjugation, but the surface charge of FA-modified nanoliposomes likely plays an important role in how drug-loaded nanoliposomes interact with cells and consequently their cytotoxicity. Cationic liposomes have been reported to generally exhibit higher cellular uptake,

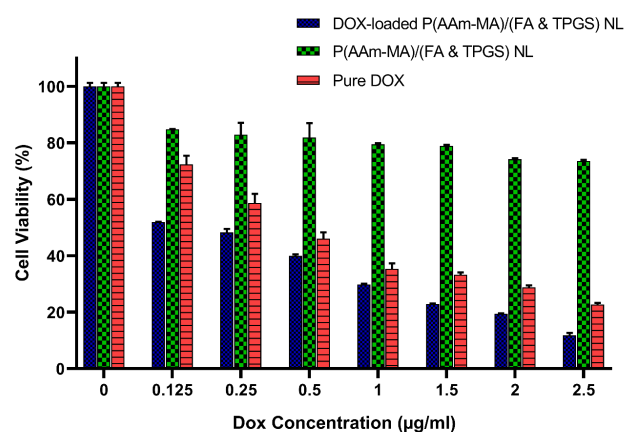


**Figure 13.** The *in vitro* cell viability in MCF-7 cells after incubation of P(AAm-MA)/(FA & TPGS) nanoliposome (NL), pure DOX drug, and DOX-loaded P(AAm-MA)/(FA & TPGS) NL at different concentrations for 48 h. Data are presented as mean ± SD (n=3). Statistical significance of the results was assessed using a two-way analysis of variance (ANOVA) and the *P* values from this analysis are reported. The interaction between concentrations and formulations (Pure DOX, DOX-loaded P(AAm-MA)/(FA & TPGS) NL, P(AAm-MA)/(FA & TPGS) NL) was significant (*P*<0.0001). The effect of concentration alone (*P*<0.0001) and different formulations (*P*<0.0001) was also significant. All of the data were analyzed using GraphPad Prism 8 software

meaning they are more readily absorbed by cancer cells. The electrostatic attraction between the positively charged liposomes and the negatively charged cell membrane facilitates this uptake.<sup>38</sup> In this study, the prepared DOX-loaded P(AAm-MA)/(FA & TPGS) NL with a positively charged polymer coating exhibits higher cellular uptake and increased cytotoxicity in MCF-7 tumor cells. This phenomenon can be attributed to the electrostatic attraction between the positively charged polymer-coated nanoliposome and the negatively charged cell membrane. This attraction causes absorptive endocytosis, in which the cell internalizes the DOX-loaded P(AAm-MA)/(FA & TPGS) NL to neutralize the surface charge. So, the DOX-loaded P(AAm-MA)/(FA & TPGS) NL can be a suitable choice for inhibiting MCF-7 cancer cells.

### Cellular Uptake Study

The FA receptors are over-expressed in MCF-7 tumor cells.<sup>35</sup> So, FA-modified nano liposomal carriers could be a suitable choice for targeted drug delivery. The *in vitro* cellular uptake of free DOX and DOX-loaded P(AAm-MA)/(FA & TPGS) NL against MCF-7 cells after 180 min is shown in Figure 14a and b, respectively. As shown in Figure 14, for free DOX, slight red fluorescence can be noticed in MCF-7 cells after 180 min, while for the targeted DOX-loaded P(AAm-MA)/(FA & TPGS) NL, a strong red fluorescence is observed after 180 min. This phenomenon indicates a higher DOX uptake in DOX-loaded P(AAm-MA)/(FA & TPGS) NL compared to free DOX formulation. This result states that the modified P(AAm-MA)/(FA & TPGS) NL can be a good choice for use in the targeted delivery of antitumor drugs because of its enhanced cellular uptake via FA receptor-mediated endocytosis. Although the current data suggest a possible FA receptor-mediated endocytosis pathway, this mechanism has not been directly confirmed. Further investigation, such as studies involving specific receptor-blocking antibodies, would be necessary to directly verify the involvement of FA receptors in the internalization process.

The intracellular uptake of prepared P(AAm-MA)/(FA & TPGS) NL is displayed schematically in Figure 3. While our team focused on targeting receptors of tumor cells by FA conjugation, the surface charge of FA-modified nanoliposomes likely plays an important role in how the liposomes interact with cells and how

efficiently they are absorbed.

Positively charged nanoliposomes tend to interact more easily with negatively charged cell membranes, facilitating their binding and entry into cells. This phenomenon is a key factor in cellular uptake. The positive charge can enhance cellular uptake through a process called absorptive endocytosis, in which the cell actively internalizes the nanoliposome to neutralize the surface charge.<sup>38</sup> The positive surface charge of P(AAm-MA)/(FA & TPGS) NL, along with targeting tumor cell receptors by FA, likely contributes to the enhanced cellular uptake and cytotoxicity observed in this study.

Although the positive charge enhances cellular uptake, it may also have an impact on the biodistribution of liposomes, which could be further investigated in future studies. The positive charge may lead to faster clearance from the bloodstream, resulting in reduced circulation time.<sup>39</sup> In this study, this effect is potentially reduced by coating the prepared NL with FA-containing polymer, which can increase the circulation time.

### Conclusion

A positively charged P(AAm-MA)/(FA & TPGS) copolymer has been synthesized and used to coat the negative surface of the lecithin-based NL in order to prepare the developed P(AAm-MA)/(FA & TPGS) NL. The prepared FA-modified P(AAm-MA)/(FA & TPGS) NL is designed for use in the targeted delivery of antitumor DOX drug into the cancerous cells. The DOX-loaded P(AAm-MA)/(FA & TPGS) NL successfully controlled MCF-7 tumor cell growth because of its enhanced cellular uptake via FA receptor-mediated endocytosis. Also, the DOX-loaded P(AAm-MA)/(FA & TPGS) NL exhibited more cytotoxicity than pure DOX. As a result, this P(AAm-MA)/(FA & TPGS) NL represents a suitable candidate for targeted internalization of antitumor therapeutic drugs to cancer cells. The current study is limited by its *in vitro* nature, and the findings cannot be directly generalized to a living organism. So, future *in vivo* studies are essential for understanding how the prepared drug delivery system behaves in living organisms. In particular, future studies should focus on conducting experiments in animal models to evaluate the effects of the prepared drug delivery system on the whole organism. If animal studies are promising, the next step would be to conduct human clinical trials to determine the safety and

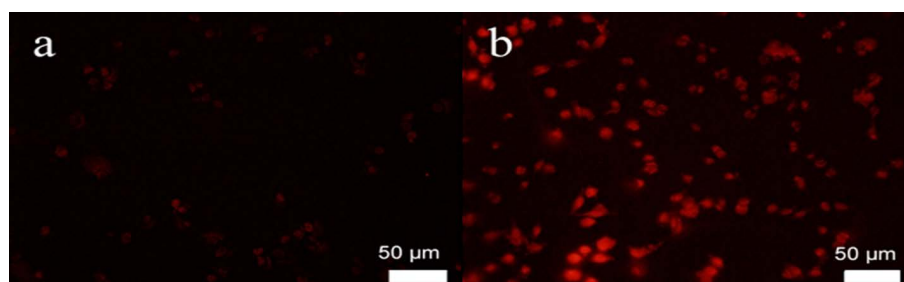


**Figure 14.** The *in vitro* cellular uptake of a) free DOX and b) targeted DOX-loaded P(AAm-MA)/(FA & TPGS) nanoliposome (NL) against MCF-7 cells after 180 min

efficacy of the prepared targeted drug delivery system in humans.

#### Acknowledgements

We wish to acknowledge Urmia University for spiritually and financially support of this research study.

#### Authors' Contribution

Conceptualization: Farzaneh Sadrykia, Peyman Najafi Moghadam.  
Data curation: Farzaneh Sadrykia.

Formal analysis: Farzaneh Sadrykia, Peyman Najafi Moghadam, Hamed Hamishehkar.

Funding acquisition: Peyman Najafi Moghadam.

Investigation: Farzaneh Sadrykia.

Methodology: Farzaneh Sadrykia.

Project administration: Peyman Najafi Moghadam.

Resources: Peyman Najafi Moghadam, Hamed Hamishehkar.

Software: Farzaneh Sadrykia.

Supervision: Peyman Najafi Moghadam.

Validation: Peyman Najafi Moghadam.

Visualization: Farzaneh Sadrykia.

Writing-original draft: Farzaneh Sadrykia.

Writing-review & editing: Peyman Najafi Moghadam, Hamed Hamishehkar.

#### Competing Interests

None.

#### Ethical Approval

Not applicable.

#### Funding

This study was self-funded by the authors.

#### References

- Mansoori B, Mohammadi A, Davudian S, Shirjang S, Baradaran B. The different mechanisms of cancer drug resistance: a brief review. *Adv Pharm Bull.* 2017;7(3):339-48. doi: [10.15171/apb.2017.041](https://doi.org/10.15171/apb.2017.041)
- Kumar K, Umapathi R, Mor S, Ghoreishian SM, Tiwari JN, Ramezani Farani M, et al. Manipulation of thermoresponsive polymers using biomolecules. *ACS Appl Polym Mater.* 2023;5(5):3181-200. doi: [10.1021/acsapm.2c02162](https://doi.org/10.1021/acsapm.2c02162)
- Hossen S, Hossain MK, Basher MK, Mia MN, Rahman MT, Uddin MJ. Smart nanocarrier-based drug delivery systems for cancer therapy and toxicity studies: A review. *J Adv Res.* 2019;15:1-18. doi: [10.1016/j.jare.2018.06.005](https://doi.org/10.1016/j.jare.2018.06.005)
- Namazi H, Pooresmaeil M, Salehi R. Construction of a new dual-drug delivery system based on stimuli-responsive copolymer functionalized D-mannose for chemotherapy of breast cancer. *Eur Polym J.* 2023;188:111958. doi: [10.1016/j.eurpolymj.2023.111958](https://doi.org/10.1016/j.eurpolymj.2023.111958)
- Hu L, Xiong C, Wei G, Yu Y, Li S, Xiong X, et al. Stimuli-responsive charge-reversal MOF@polymer hybrid nanocomposites for enhanced co-delivery of chemotherapeutics towards combination therapy of multidrug-resistant cancer. *J Colloid Interface Sci.* 2022;608(Pt 2):1882-93. doi: [10.1016/j.jcis.2021.10.070](https://doi.org/10.1016/j.jcis.2021.10.070)
- Zhang D, Zhang J, Li Q, Tian H, Zhang N, Li Z, et al. pH-and enzyme-sensitive IR820-paclitaxel conjugate self-assembled nanovehicles for near-infrared fluorescence imaging-guided chemo-photothermal therapy. *ACS Appl Mater Interfaces.* 2018;10(36):30092-102. doi: [10.1021/acsami.8b09098](https://doi.org/10.1021/acsami.8b09098)
- Wang Y, Shim MS, Levinson NS, Sung HW, Xia Y. Stimuli-responsive materials for controlled release of theranostic agents. *Adv Funct Mater.* 2014;24(27):4206-20. doi: [10.1002/adfm.201400279](https://doi.org/10.1002/adfm.201400279)
- Veisheh O, Gunn JW, Zhang M. Design and fabrication of magnetic nanoparticles for targeted drug delivery and imaging. *Adv Drug Deliv Rev.* 2010;62(3):284-304. doi: [10.1016/j.addr.2009.11.002](https://doi.org/10.1016/j.addr.2009.11.002)
- Ghorbani M, Hamishehkar H. Redox-responsive smart nanogels for intracellular targeting of therapeutic agents: applications and recent advances. *J Drug Target.* 2019;27(4):408-22. doi: [10.1080/1061186x.2018.1514041](https://doi.org/10.1080/1061186x.2018.1514041)
- Vinothini K, Rajendran NK, Ramu A, Elumalai N, Rajan M. Folate receptor targeted delivery of paclitaxel to breast cancer cells via folic acid conjugated graphene oxide grafted methyl acrylate nanocarrier. *Biomed Pharmacother.* 2019;110:906-17. doi: [10.1016/j.biopha.2018.12.008](https://doi.org/10.1016/j.biopha.2018.12.008)
- Qindeel M, Khan D, Ahmed N, Khan S, Asim Ur Rehman. Surfactant-free, self-assembled nanomicelles-based transdermal hydrogel for safe and targeted delivery of methotrexate against rheumatoid arthritis. *ACS Nano.* 2020;14(4):4662-81. doi: [10.1021/acsnano.0c00364](https://doi.org/10.1021/acsnano.0c00364)
- Huang L, Song J, Chen B. A novel targeting drug carrier to deliver chemical bonded and physical entrapped anti-tumor drugs. *Int J Pharm.* 2014;466(1-2):52-7. doi: [10.1016/j.ijpharm.2014.03.006](https://doi.org/10.1016/j.ijpharm.2014.03.006)
- Nezhad-Mokhtari P, Ghorbani M, Mahmoodzadeh F. Smart co-delivery of 6-mercaptopurine and methotrexate using disulphide-based PEGylated-nanogels for effective treatment of breast cancer. *New J Chem.* 2019;43(30):12159-67. doi: [10.1039/c9nj02470k](https://doi.org/10.1039/c9nj02470k)
- Kim JE, Shin JY, Cho MH. Magnetic nanoparticles: an update of application for drug delivery and possible toxic effects. *Arch Toxicol.* 2012;86(5):685-700. doi: [10.1007/s00204-011-0773-3](https://doi.org/10.1007/s00204-011-0773-3)
- Decatris MP, Sundar S, O'Byrne KJ. Platinum-based chemotherapy in metastatic breast cancer: current status. *Cancer Treat Rev.* 2004;30(1):53-81. doi: [10.1016/s0305-7372\(03\)00139-7](https://doi.org/10.1016/s0305-7372(03)00139-7)
- Azarian M, Ramezani Farani M, Cho WC, Asgharzadeh F, Yang YJ, Moradi Binabaj M, et al. Advancements in colorectal cancer treatment: the role of metal-based and inorganic nanoparticles in modern therapeutic approaches. *Pathol Res Pract.* 2024;264:155706. doi: [10.1016/j.prp.2024.155706](https://doi.org/10.1016/j.prp.2024.155706)
- Sadeghzadeh F, Motavalizadehkakhky A, Mehrzad J, Zhiani R, Homayouni Tabrizi M. Folic acid conjugated-chitosan modified nanostructured lipid carriers as promising carriers for delivery of umbelliprenin to cancer cells: in vivo and in vitro. *Eur Polym J.* 2023;186:111849. doi: [10.1016/j.eurpolymj.2023.111849](https://doi.org/10.1016/j.eurpolymj.2023.111849)
- Azarian M, Ramezani Farani M, Zare I, Imani M, Kumar K, Huh YS, et al. Functionalized porphyrinsomes and porphyrin-based nanomaterials for cancer therapy. In: Barabadi H, Mostafavi E, Mustansar Hussain C, eds. *Functionalized Nanomaterials for Cancer Research.* Academic Press; 2024. p. 329-44. doi: [10.1016/b978-0-443-15518-5.00002-1](https://doi.org/10.1016/b978-0-443-15518-5.00002-1)
- Ramezani Farani M, Zare I, Mirshafiei M, Gholami A, Zhang M, Pishbin E, et al. Graphene oxide-engineered chitosan nanoparticles: synthesis, properties, and antibacterial activity for tissue engineering and regenerative medicine. *Chem Eng J.* 2025;509:160852. doi: [10.1016/j.cej.2025.160852](https://doi.org/10.1016/j.cej.2025.160852)
- Ramezani Farani M, Azarian M, Heydari Sheikh Hossein H, Abdolvahabi Z, Mohammadi Abgarmi Z, Moradi A, et al. Folic acid-adorned curcumin-loaded iron oxide nanoparticles for cervical cancer. *ACS Appl Bio Mater.* 2022;5(3):1305-18. doi: [10.1021/acsabm.1c01311](https://doi.org/10.1021/acsabm.1c01311)
- Mohandes F, Dehghani H, Angizi S, Ramedani A, Dolatyar B, Ramezani Farani M, et al. Magneto-fluorescent contrast agents based on carbon Dots@Ferrite nanoparticles for tumor imaging. *J Magn Magn Mater.* 2022;561:169686. doi: [10.1016/j.jmmm.2022.169686](https://doi.org/10.1016/j.jmmm.2022.169686)
- Ehsanimehr S, Najafi Moghadam P, Dehaen W, Shafiei-

- Irannejad V. PEI grafted Fe<sub>3</sub>O<sub>4</sub>@SiO<sub>2</sub>@SBA-15 labeled FA as a pH-sensitive mesoporous magnetic and biocompatible nanocarrier for targeted delivery of doxorubicin to MCF-7 cell line. *Colloids Surf A Physicochem Eng Asp*. 2021;615:126302. doi: [10.1016/j.colsurfa.2021.126302](https://doi.org/10.1016/j.colsurfa.2021.126302)
23. Kesim H, Rzaev ZM, Dinçer S, Pişkin E. Functional bioengineering copolymers. II. Synthesis and characterization of amphiphilic poly(N-isopropyl acrylamide-co-maleic anhydride) and its macrobranched derivatives. *Polymer (Guildf)*. 2003;44(10):2897-909. doi: [10.1016/s0032-3861\(03\)00177-0](https://doi.org/10.1016/s0032-3861(03)00177-0)
24. Anbharasi V, Cao N, Feng SS. Doxorubicin conjugated to D-alpha-tocopheryl polyethylene glycol succinate and folic acid as a prodrug for targeted chemotherapy. *J Biomed Mater Res A*. 2010;94(3):730-43. doi: [10.1002/jbm.a.32734](https://doi.org/10.1002/jbm.a.32734)
25. Jalali N, Moztarzadeh F, Mozafari M, Asgari S, Motevalian M, Naghavi Alhosseini S. Surface modification of poly(lactide-co-glycolide) nanoparticles by d-α-tocopheryl polyethylene glycol 1000 succinate as potential carrier for the delivery of drugs to the brain. *Colloids Surf A Physicochem Eng Asp*. 2011;392(1):335-42. doi: [10.1016/j.colsurfa.2011.10.012](https://doi.org/10.1016/j.colsurfa.2011.10.012)
26. Lei M, Ma G, Sha S, Wang X, Feng H, Zhu Y, et al. Dual-functionalized liposome by co-delivery of paclitaxel with sorafenib for synergistic antitumor efficacy and reversion of multidrug resistance. *Drug Deliv*. 2019;26(1):262-72. doi: [10.1080/10717544.2019.1580797](https://doi.org/10.1080/10717544.2019.1580797)
27. Asghari Fesendouz S, Hamishehkar H, Alizadeh E, Rahbarghazi R, Akbarzadeh A, Yousefi S, et al. Bactericidal activity and biofilm eradication of *Pseudomonas aeruginosa* by liposome-encapsulated piperacillin/tazobactam. *BioNanoScience*. 2024;15(1):87. doi: [10.1007/s12668-024-01699-0](https://doi.org/10.1007/s12668-024-01699-0)
28. Dianat-Moghadam H, Heidarifard M, Jahanban-Esfahlan R, Panahi Y, Hamishehkar H, Pouremamali F, et al. Cancer stem cells-emanated therapy resistance: Implications for liposomal drug delivery systems. *J Control Release*. 2018;288:62-83. doi: [10.1016/j.jconrel.2018.08.043](https://doi.org/10.1016/j.jconrel.2018.08.043)
29. Zhou S, Zhang T, Peng B, Luo X, Liu X, Hu L, et al. Targeted delivery of epirubicin to tumor-associated macrophages by sialic acid-cholesterol conjugate modified liposomes with improved antitumor activity. *Int J Pharm*. 2017;523(1):203-16. doi: [10.1016/j.ijpharm.2017.03.034](https://doi.org/10.1016/j.ijpharm.2017.03.034)
30. Mallick S, Thuy LT, Lee S, Park JI, Choi JS. Liposomes containing cholesterol and mitochondria-penetrating peptide (MPP) for targeted delivery of antimycin A to A549 cells. *Colloids Surf B Biointerfaces*. 2018;161:356-64. doi: [10.1016/j.colsurfb.2017.10.052](https://doi.org/10.1016/j.colsurfb.2017.10.052)
31. Naeimifar A, Ahmad Nasrollahi S, Akbari Javar H, Nassiri Kashani M, Firooz A, Rouini M. Designing a topical nanoliposomal formulation of ruxolitinib phosphate. *Pharm Sci*. 2022;29(1):75-83. doi: [10.34172/ps.2022.17](https://doi.org/10.34172/ps.2022.17)
32. Shabanlouei R, Najafi Moghadam P, Movagharneshad N, Fareghi AR. Template polymerization of aniline in presence of poly(acrylamide-co-maleic acid) for preparation of conductive polymers. *Polym Sci Ser B*. 2016;58(5):574-9. doi: [10.1134/s1560090416050092](https://doi.org/10.1134/s1560090416050092)
33. Tsend-Ayush A, Zhu X, Ding Y, Yao J, Yin L, Zhou J, et al. Lactobionic acid-conjugated TPGS nanoparticles for enhancing therapeutic efficacy of etoposide against hepatocellular carcinoma. *Nanotechnology*. 2017;28(19):195602. doi: [10.1088/1361-6528/aa66ba](https://doi.org/10.1088/1361-6528/aa66ba)
34. Amjadi S, Almasi H, Hamishehkar H, Alizadeh Khaledabad M, Lim LT. Cationic inulin as a new surface decoration hydrocolloid for improving the stability of liposomal nanocarriers. *Colloids Surf B Biointerfaces*. 2022;213:112401. doi: [10.1016/j.colsurfb.2022.112401](https://doi.org/10.1016/j.colsurfb.2022.112401)
35. Yin M, Bao Y, Gao X, Wu Y, Sun Y, Zhao X, et al. Redox/pH dual-sensitive hybrid micelles for targeting delivery and overcoming multidrug resistance of cancer. *J Mater Chem B*. 2017;5(16):2964-78. doi: [10.1039/c6tb03282f](https://doi.org/10.1039/c6tb03282f)
36. Nsairat H, Khater D, Sayed U, Odeh F, Al Bawab A, Alshaer W. Liposomes: structure, composition, types, and clinical applications. *Heliyon*. 2022;8(5):e09394. doi: [10.1016/j.heliyon.2022.e09394](https://doi.org/10.1016/j.heliyon.2022.e09394)
37. Sriwidodo, Umar AK, Wathoni N, Zothantluanga JH, Das S, Luckanagul JA. Liposome-polymer complex for drug delivery system and vaccine stabilization. *Heliyon*. 2022;8(2):e08934. doi: [10.1016/j.heliyon.2022.e08934](https://doi.org/10.1016/j.heliyon.2022.e08934)
38. Li L, Yang Q, Zhou Z, Zhong J, Huang Y. Doxorubicin-loaded, charge reversible, folate modified HPMA copolymer conjugates for active cancer cell targeting. *Biomaterials*. 2014;35(19):5171-87. doi: [10.1016/j.biomaterials.2014.03.027](https://doi.org/10.1016/j.biomaterials.2014.03.027)
39. Triantafyllopoulou E, Pippa N, Demetzos C. Protein-liposome interactions: the impact of surface charge and fluidisation effect on protein binding. *J Liposome Res*. 2023;33(1):77-88. doi: [10.1080/08982104.2022.2071296](https://doi.org/10.1080/08982104.2022.2071296)